Blood oxygenation level-dependent contrast response functions identify mechanisms of covert attention in early visual areas

Xiangrui Li[†], Zhong-Lin Lu[†‡], Bosco S. Tjan[†], Barbara A. Dosher[§], and Wilson Chu[†]

[†]Dana and David Dornsife Cognitive Neuroscience Imaging Center and Department of Psychology, University of Southern California, Los Angeles, CA 90089; and [§]Department of Cognitive Sciences, University of California, Irvine, CA 92697

Communicated by Richard M. Shiffrin, Indiana University, Bloomington, IN, February 11, 2008 (received for review November 23, 2007)

Covert attention can lead to improved performance in perceptual tasks. The neural and functional mechanisms of covert attention are still under investigation. Using both rapid event-related and mixed designs, we measured the blood oxygenation level-dependent functional MRI contrast response functions over the full range of contrast (0–100%) in the retinotopically defined early visual areas (V1, V2, V3, V3A, and V4) in humans. Covert attention increased both the baseline activities and contrast gains in the five cortical areas. The effect on baseline can be decomposed into a transient trial-by-trial component and a component across an entire attention block. On average, increase in contrast gain accounted for ≈88.0%, 28.5%, 12.7%, 35.9%, and 25.2% of the trial-by-trial effects of attention in the five areas, respectively, and 22.2%, 12.8%, 7.4%, 19.7%, and 17.3% of the total effects of attention in those areas, consistent with single-unit findings in V4 and MT. The results provide strong evidence for a stimulus enhancement mechanism of attention as demonstrated in various behavioral studies.

contrast gain | increased baseline | response gain | stimulus enhancement

Covert attention can lead to improved performance accuracy and response time (1, 2). Since the initial discovery that attention increases the blood oxygenation level-dependent (BOLD) responses in early visual areas (3–9), a large number of new studies have further documented many interesting effects of attention in the visual pathway, including attentional modulation of the BOLD responses in the lateral geniculate nucleus (10), increased BOLD activities in the visual cortical areas corresponding to the attended spatial location in the absence of visual stimulation (6, 11, 12), different effects of endogenous and exogenous attention (13, 14), and topographic maps of visual spatial attention in parietal cortex (15). How attention enhances visual stimuli in early visual cortical areas, however, remains unclear. We attempt to address this fundamental question in this study.

There are three potential mechanisms underlying the increased BOLD responses in early visual areas (Fig. 1): increased contrast gain, increased response gain, and increased baseline activity. Formulated in terms of the impact of attention on contrast response functions (CRFs), these three mechanisms have distinct behavioral and functional significance. In the behavioral domain, a theoretical framework based on analyses of human observers distinguishes three mechanisms of attention: stimulus enhancement, external noise exclusion, and nonlinearity change (16, 17). Whereas an increase in baseline activity need not contribute to improved discrimination and cannot be observed in psychophysical studies (18), increased contrast gain (18, 19) is related to behaviorally identified stimulus enhancement in a discrimination task, and response gain corresponds to nonlinearity changes observed behaviorally (20). Because most of the functional MRI (fMRI) attention studies used a single stimulus contrast, the observed increases of the BOLD response are compatible with any of the three potential modulations of

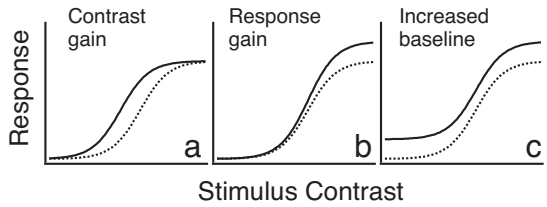

Fig. 1. Three potential mechanisms of covert attention. (*a*) Contrast gain. (*b*) Response gain. (*c*) Increased baseline activity.

CRFs. To understand the mechanism underlying the increased BOLD responses, it is necessary to study the impact of covert attention over a wide range of stimulus contrasts.

CRFs—mean firing rate versus signal stimulus contrast—characterize one of the most fundamental properties of visual neurons (21). In fMRI research, a number of retinotopy techniques have been developed to demarcate individual early visual areas in humans (22, 23). BOLD CRFs can then be obtained by manipulating stimulus contrast and observing the summed BOLD responses in individual visual cortical areas (24–28). In this study, we investigated attentional modulation of the BOLD CRFs in five early visual areas of the human brain.

Attentional modulation of CRFs has been examined in single-unit recordings, human psychophysics, and fMRI. Martinez-Trujillo and Treue (29) found that attention increased contrast gain in monkey MT. Recording from monkey V4, Reynolds *et al.* (19) and Williford and Maunsell (18) both found that attention increased baseline spontaneous activity but disagreed on whether attention also increased the effective contrast (19) or response gain (18). In psychophysical studies, several findings have also been reported, supporting response gain (30), contrast gain at an early stage followed by response gain at a later stage for endogenous attention (31), or contrast gain for endogenous attention and a mixture of response gain and contrast gain for exogenous attention (32). Finally, using both contrast and speed discrimination in an fMRI study, Buracas and Boynton (25) found that the modulation of the BOLD responses in early visual areas (V1, V2, V3, and MT+) by spatial attention was similar across stimulus contrasts, consistent with an increased baseline mechanism.

The current study complements that of Buracas and Boynton (25). After obtaining the retinotopies of the observers, BOLD

Author contributions: Z.-L.L., B.S.T., and B.A.D. designed research. X.L., Z.-L.L., and W.C. performed research; X.L., Z.-L.L., and B.S.T. analyzed data; and X.L., Z.-L.L., B.S.T., and B.A.D. wrote the paper.

The authors declare no conflict of interest.

‡To whom correspondence should be addressed. E-mail: zhonglin@usc.edu.

This article contains supporting information online at www.pnas.org/cgi/content/full/0801390105/DCSupplemental.

responses were collected from V1, V2, V3, V3A, and V4. Experiment 1 used a combination of mixed and event-related designs to measure the BOLD response as functions of grating contrast and attention and to separate the trial-by-trial and block effects of attention. Experiment 2 investigated effects of general task difficulty on the BOLD response, in which the precision of the orientation discrimination task was manipulated for gratings at a constant contrast. The joint results of these experiments enabled us to compare the BOLD CRFs in the attended and unattended conditions and identify the mechanisms of covert attention in early visual cortical areas.

The study differs from that of Buracas and Boynton (25) in several important ways:

1. A wider range of stimulus contrast (0–100%) and very brief stimulus duration (100 ms). The zero- and low-contrast conditions (1–3%) are critical for assessing baseline shifts and contrast gain, whereas the high contrasts (e.g., 100%) are important for evaluating response gain. The very brief stimulus duration is what is typically used in psychophysical studies, so our results may be more directly related to behavioral studies.
2. Explicit evaluation of the effects of task difficulty on the BOLD response. To control for potential effects of general task difficulty, Buracas and Boynton (25) covaried contrast and speed increments with the tested contrast levels to keep subjects performing at a constant level. The observed BOLD CRFs could have been confounded by variations of stimulus properties other than contrast. By showing that the precision of the orientation discrimination task had no effect on the BOLD response, we need only to manipulate stimulus contrast when measuring the BOLD CRFs.
3. Event-related and mixed designs. A combination of event-related and mixed designs is necessary to separate the transient trial-by-trial effects of attention on the BOLD CRFs from those of the attentional state within a block of attended trials. In comparison, a block design measures the combined trial-by-trial and longer-term block effects of attention. The trial-to-trial variations of stimulus contrast in the event-related and mixed designs also reduced the differential effects of contrast adaptation on the BOLD CRFs, a potential issue in ref. 25.

Results

Experiment 1: BOLD CRFs. Experiment 1A used interleaving blocks of attended and unattended trials within each fMRI run, with four different contrast levels tested within each block of an event-related design. This mixed design simultaneously measures the effects of attention over a block of trials and for individual trials. Experiment 1B used a pure event-related design to test six contrast levels, rather than four, to better estimate the CRF, with attention manipulated across runs. The two subexperiments yield quantitatively identical results after removing the block effect of attention from Experiment 1A, allowing combination of the data from the two subexperiments.

Behavioral responses. Performance accuracies and response times in the central and the peripheral tasks are shown in Fig. 2*a* as functions of the grating contrast. The accuracy data from Experiments 1A and 1B did not differ significantly and are combined. In the unattended condition, central letter identification accuracy was 86.9 ± 1.1% and was virtually identical across grating contrasts. The accuracy of grating orientation judgments increased significantly from 53% to 94% correct as its contrast increased from 0% to 100%. The mean response times did not significantly differ between the central and the peripheral tasks. Eye movements were stable across conditions [supporting information (SI) *Text*].

Trial-by-trial and block effects of attention. The analysis of Experiment 1A estimated a block factor in the general linear model in addition to the trial-by-trial hemodynamic response function (HRF) predictors. The block factors estimated that the BOLD responses to gratings in the attended block were increased by 0.099 ± 0.006, 0.098 ± 0.008, 0.092 ± 0.009, 0.075 ± 0.005, and 0.047 ± 0.008 in units of percent signal change in V1, V2, V3, V3A, and V4, respectively. This corresponds to a baseline change across the entire block of attended trials.

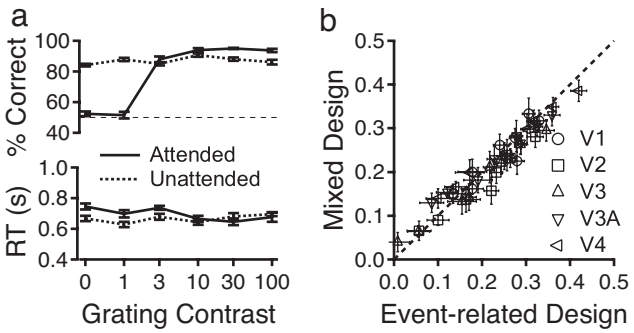

Fig. 2. Behavioral responses and the relationship of the trial-by-trial BOLD amplitudes in the mixed and event-related designs. (*a*) Average performance accuracies and response times from Experiments 1A and 1B. (*b*) Scatter plot of the trial-by-trial BOLD response amplitudes from Experiment 1A (mixed design) versus those from Experiment 1B (event-related design) in the four common contrast conditions.

The BOLD responses from Experiments 1A and 1B are virtually identical ($r = 0.9649$; $P > 0.7$) when the trial-by-trial amplitudes are plotted against each other (Fig. 2*b*). The high correlation between the BOLD responses estimated from the two different designs provides important evidence for the reliability of the data. It also validates the data analysis procedure used in Experiment 1A. We combined the trial-by-trial data from Experiments 1A and 1B in subsequent analyses.

Identifying mechanisms of attention. The amplitudes of trial-by-trial BOLD responses in all the contrast and attention conditions, averaged across subjects, are plotted as functions of signal contrast (the BOLD CRF) in Fig. 3*b*. The patterns of results from individual subjects are similar. The Naka–Rushton equation was fit to these BOLD CRFs in each cortical region (33, 34):

$$R(c) = b + \frac{R_{\max} c^2}{c_{50}^2 + c^2}, \qquad [1]$$

where c is the contrast of the grating, b is the baseline activity, c_{50} denotes the contrast at which the response reaches half of its

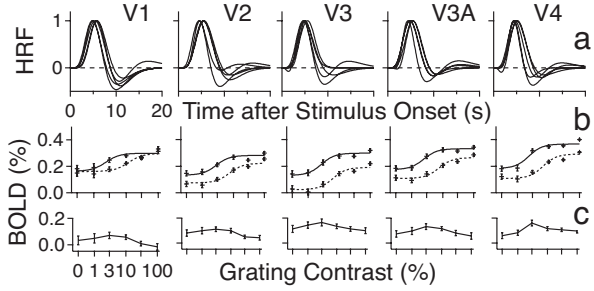

Fig. 3. HRFs and CRFs. (*a*) Normalized HRF for each visual area. Each subject is represented by one curve with peak amplitude normalized to 1.0. (*b*) BOLD CRFs. The smooth curves are the predictions of the best fitting model. The solid and dotted curves represent attended and unattended conditions, respectively. (*c*) Difference of the contrast responses in the attended and unattended conditions.

Table 1. Parameters of the best fitting Naka–Rushton model

		Unattended		Attended	
Visual area	R_{max}	c_{50}	b	c_{50}	b
V1	0.13 ± 0.02	11.60 ± 3.90	0.16 ± 0.03	2.18 ± 0.52	0.16 ± 0.03
V2	0.14 ± 0.01	7.04 ± 1.20	0.08 ± 0.02	2.52 ± 0.36	0.13 ± 0.02
V3	0.17 ± 0.01	6.16 ± 0.92	0.03 ± 0.01	2.55 ± 0.33	0.14 ± 0.02
V3A	0.15 ± 0.01	8.06 ± 1.35	0.11 ± 0.03	2.43 ± 0.34	0.17 ± 0.02
V4	0.18 ± 0.01	6.40 ± 1.41	0.12 ± 0.02	2.27 ± 0.24	0.19 ± 0.03

maximum dynamic range, and R_{max} is the maximum response above the baseline.

The mechanisms of attention in the early visual areas were tested with a nested model lattice of eight models (*SI Text*). In the most saturated model, all parameters of the Naka–Rushton equation (b, c_{50}, and R_{max}) are changed between the attended and unattended conditions. In the most reduced model, the attention conditions do not differ and share all parameters of the Naka–Rushton equation. Intermediate models sharing some but not all parameters were also considered. Statistical tests of nested models identify the simplest model that accounts for the data: an increase of b in the attended condition signifies increased baseline activity; a decrease of c_{50} signifies contrast gain; and an increase of R_{max} indicates response gain.

In all of the five cortical areas, the best fitting Naka–Rushton model included both contrast gain and increased baseline activity. The model, shown as smooth curves in Fig. 3*b*, accounted for 96.3% of the variance in the data. This model is statistically as good as the most saturated model [$F(5,30) = 1.14, P > 0.30$] and superior to all of its reduced versions ($P < 0.005$). In comparison, the response-gain-only model is significantly inferior to the full model [83.9% of variance, $F(10,30) = 12.70, P < 0.00001$], as were all of the intermediate models that included response gain but not at least one of the other two mechanisms ($P < 0.005$). A bootstrap procedure with 1,000,000 iterations was used to evaluate the effect of individual differences on model selection (*SI Text*). The contrast-gain-plus-increased-baseline model was the best fitting model 85.3% of the time, the baseline-alone model was the best 6.26% of the time, and the contrast-gain-alone model was the best 0.42% of the time. Importantly, the pure response-gain model was never the best fitting model. These results convincingly support the contrast-gain-plus-increased-baseline model as the best account of our data.

The parameters of the best fitting contrast-gain-plus-increased-baseline model and their standard deviations are listed in Table 1. Attention increased the baseline activity by 0.004, 0.057, 0.112, 0.059, and 0.078 in units of percent signal change in V1, V2, V3, V3A, and V4, respectively. These baseline increases occur within the trial duration and are over and above the block effects of attention. The contrast-gain effects [$c_{50}(un)/c_{50}(att)$] in these regions were 5.31, 2.79, 2.42, 3.32, and 2.81, respectively.

Fig. 3*c* plots the difference between the BOLD contrast responses with and without attention. All of the difference functions exhibit a bump in the intermediate contrast conditions, characteristic of the contrast-gain mechanism of attention. An estimated 88.0%, 28.5%, 12.7%, 35.9%, and 25.2% (mean = 38.1%) of the attention effects in areas V1, V2, V3, V3A, and V4, respectively, were accounted for by contrast gain, and the rest were accounted for by increased baseline activities. It is remarkable that V1, unlike other area, has within-trial attention effects dominated by contrast gain.

If we combine trial-by-trial and block effects of attention, then 77.8%, 87.2%, 92.6%, 80.3%, and 82.7% of the total attention effects are accounted for by increased baseline activities; 22.2%, 12.8%, 7.4%, 19.7%, and 17.3% (mean = 15.9%) are accounted for by contrast gain. In previous fMRI studies based on block designs (25), trial-by-trial and block effects of attention were not separately estimated. The observed effects of attention de facto combined trial-by-trial and block factors of covert attention and so estimated mostly baseline differences.

Effects of attention at other eccentricities are also estimated (*SI Text*). In general, attending to the grating reduced the BOLD response in foveal regions and increased the BOLD responses in cortical areas near the regions of interest (ROIs) corresponding to the signal gratings used in this study.

Experiment 2: Effect of Task Difficulty on the BOLD Response. Characterizing CRF requires measurements of the BOLD responses over a wide range of signal contrast, corresponding to a wide range of performance accuracies. Several fMRI studies have suggested that task difficulty could change the BOLD responses (12, 35–37). Buracas and Boynton (25) approached the issue by adjusting task precision in distinct contrast conditions to equate task difficulty (accuracy), thus covarying the variable of interest, contrast, with other stimulus properties, such as speed or contrast increments. Instead, we chose to explicitly investigate the effects of task difficulty on the BOLD responses by manipulating the precision of orientation discrimination from 45 ± 1° to 45 ± 10° while keeping the contrast of the stimulus constant; 1.9% and 19% contrast were tested separately.

Fig. 4 shows the BOLD response amplitude as functions of the discrimination precision. The BOLD response was unchanged by task precision in all five early visual areas, for both grating contrast levels in both attention conditions (all $P > 0.50$), although behavioral accuracy ranged from 50.8% to 72.0% at 1.9% contrast and 65.2% to 98.6% correct at 19% contrast. Different accuracy levels resulted in different proportions of the "correct" vs. "incorrect" feedback, so the results also rule out feedback as an explanation for the observed effects of attention in Experiment 1.

Summary and Discussion

By measuring attentional modulation of the BOLD CRFs, we found that attention both amplifies the effective stimulus contrast and increases baseline activity. The results provide converging evidence for a stimulus enhancement mechanism of attention observed in behavioral studies and a mixture of

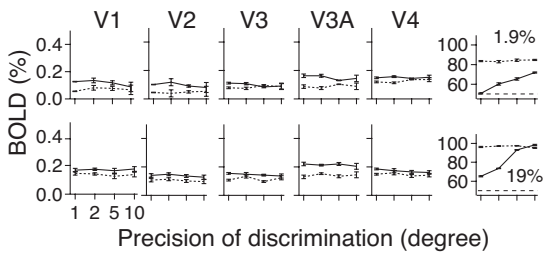

Fig. 4. Results of Experiment 2. The BOLD responses and performance accuracies are plotted in separate rows for the two grating contrast conditions.

contrast gain and increased baseline activities in single-cell studies.

Mechanisms of Covert Attention. Earlier BOLD fMRI investigations rarely manipulated stimulus contrast. These studies could document an effect of attention but could not infer the mechanisms of the attentional enhancement. Buracas and Boynton's investigation (25) found that the modulation of the BOLD responses in early visual cortical areas (V1, V2, V3, and MT+) by spatial attention does not greatly depend on stimulus contrast, consistent with a baseline shift. In the current study, increased baseline activity accounted for 12.0%, 71.5%, 87.3%, 64.1%, and 74.8% of the trial-by-trial attention effects in V1, V2, V3, V3A, and V4 and 77.8%, 87.2%, 92.6%, 80.3%, and 82.7% of the total (trial-by-trial plus block) effects of attention. Averaged across the five cortical areas, change in contrast gain accounted for ≈15.9% of the total effects of attention but were especially important in V1.

The large block and trial-to-trial baseline shifts are consistent with the observations of Buracas and Boynton (25) and may be related to reports of baseline elevations while expecting a visual target in an attended spatial location (6, 12). Using a wider contrast range and both event-related and mixed designs, we showed a clear change in contrast gain, which was either absent or undetectable in ref. 25 because only relatively high contrasts (6–75%) were used in that study.

Links to Physiology. We found that the trial-by-trial effects of attention increased the baseline BOLD activity (percent signal change) by 0.004–0.112 and increased the effective contrast of the attended stimulus by a factor of 2.4–5.3 across the five early visual areas. In comparison, Reynolds *et al.* (19) concluded that, on average, attention increased spontaneous activity by 1.1 ± 0.25 SEM spikes per second and increased the effective contrast by a factor of 1.51 for neurons in primate V4. Most importantly, both the single-unit finding by Reynolds *et al.* (19) and our BOLD fMRI results showed the same qualitative effects of attention in area V4—increased baseline activity and contrast gain. On the other hand, significant attention effects in high-stimulus-contrast conditions may be compatible with a response-gain mechanism (18). Or some single-unit data may not have the statistical power to distinguish contrast gain from response gain accounts (18). Our fMRI results favored the increased contrast gain interpretation, which is consistent with the stimulus enhancement mechanism of attention inferred from psychophysics (17, 38, 39). Our data do not show large attention effects at high contrast in addition to the baseline increase. At high contrast, Reynolds *et al.* (19) observed no attentional modulation during the first 100 ms of the neuronal response but a significant modulation in the latter part of the neural response. The timing of our stimulus (100 ms) may emphasize early responses. Differences in the experiments, such as stimulus eccentricity, may also account for some differences across the studies.

When comparing results from single-unit and fMRI studies, we must keep in mind some important methodological differences. The single-unit recording studies measured responses of cells to unattended features in the attended spatial region, whereas our BOLD fMRI study measured responses to the attended stimuli in the attended spatial region. Moreover, BOLD fMRI is an indirect measure of neuronal population activity, and the neuronal basis of the BOLD response is still under investigation (40, 41). BOLD responses to high-stimulus-contrast conditions obtained in an event-related design exhibit saturation, and single-cell responses may not show identical saturation points. Despite these caveats, the results in the distinct domains are both qualitatively and quantitatively similar.

Effects of Task Difficulty. In Experiment 2, we showed that the BOLD response was unaffected by the precision of the orientation discrimination or the general task difficulty. In a recent publication, Buracas *et al.* (42) found that the fMRI responses in V1–V3 and MT+ did not depend significantly on the task (speed discrimination versus contrast discrimination). We conclude that the BOLD responses in the early visual areas are largely functions of the stimulus contrast and not task difficulty or accuracy. Indeed, most studies that observed correlations between behavioral performance and the amplitude of the BOLD response used stimulus contrast as the independent variable so an elevated BOLD response to an increase in physical or perceived contrast is confounded with improved performance (12, 35–37).

Attentional Effects Across Visual Areas. Our BOLD fMRI results indicated that attentional modulation of the neural activities associated with stimulus contrast is very similar in five early visual areas. Other findings have argued that attention had a larger effect in higher cortical areas (6, 13, 43). However, the earlier studies tested only a single, intermediate contrast. Had we tested effects of attention at only a single intermediate contrast, we also could have concluded that attention had a larger effect in V4 than V1 or V2 (Fig. 3*b*), but this would not have been a representative result. Second, the fact that we used an event-related design while many earlier experiments used block designs might have also influenced the results. The visual areas are reciprocally interconnected (44). Block designs investigating the effect of attention at a single contrast level may be more influenced by contrast adaptation in multiple visual areas. Whether the consistency of the observed pattern in this study results across these five areas in this study is due to feed-forward or feedback activity or both between these cortical areas (19) is not addressed in the present study. Some authors suggested that the effects of attention in V1 are due to feedback connections from higher-level cortical areas. Alternatively, the larger effect of attention in BOLD fMRI relative to single-cell recording in earlier visual areas may reflect aggregate neural activity over a large number of units.

Summary. To summarize, studying attentional modulation of the full CRFs provides a framework to systematically evaluate the impact of attention on the fMRI BOLD responses in early visual areas. By measuring the magnitude of the effect of attention over a wide range of stimulus contrasts, we were able to identify two separate effects of attention: An increase in baseline activity that is unlikely to improve functional discrimination, and a contrast gain effect that could serve a functional role in stimulus processing. Increasing the contrast gain of the visual system shifts the most sensitive operating range of the system toward lower contrasts. By aligning the sharply rising portion of the CRF with lower stimulus contrasts, attention improves the visual system's ability to identify these stimuli.

Materials and Methods

Observers. Six observers (three male and three female), age 25–38 years, participated in Experiment 1 after informed consent. Three also participated in Experiment 2. The observers had either normal or corrected-to-normal vision via MRI-compatible glasses.

MRI Data Acquisition. MRI recording used a standard birdcage head-coil on a Siemens 3T MAGNETON Trio MRI system with TIM in the Dana and David Dornsife Cognitive Neuroscience Imaging Center at the University of Southern California. For each observer, sagittal images (256 × 256 × 192) of 1-mm^3 isotropic spatial resolution were obtained with a T1-weighted 3D MPRAGE sequence (TI = 1,100 ms, TR = 2,070 ms, TE = 4.14 ms, flip angle = 12°, water excitation on). BOLD activities were measured with a T2*-weighted echo-planar imaging sequence (TR = 1,000 ms, TE = 30 ms, flip angle = 65°, FOV = 224 × 224 mm, in-plane resolution = 64 × 64 pixels or 3.5 × 3.5 mm). For

retinotopy, 14 3.5-mm-thick interlaced slices (no gap) were acquired. In Experiments 1 and 2, 12 4-mm interlaced slices (no gap) were acquired. In both cases, all of the slices were oriented perpendicular to the calcarine sulcus of the observer.

Displays and Visual Stimuli. All visual stimuli were generated by a Dell PC computer running Matlab programs based on the Psychtoolbox extensions and displayed on a 32- × 24-cm rear-projection screen mounted perpendicularly to the toe-head axis in the bore of the magnet, directly above the observer's head. The video projection system consisted of a Christie DLV1280-DX three-chip DLP projector (1,024 × 768, 60 Hz), located outside of the magnet room, a lens, an iris, a wave guide, and a mirror system that delivered the images from the projector to the screen at a right angle. The background luminance of the display was set at 156 cd/m^2, with the maximum luminance at 312 cd/m^2. The projection system has a built-in linear gamma, verified with both psychophysical procedures and photometric measurements. Virtually identical psychometric thresholds were obtained from the projection system and a calibrated CRT display. Observers viewed the displays binocularly at a viewing distance of 75 cm, a full image on the screen subtended 24° (width) × 18° (height).

Wedges and rings made of flickering radial color checkerboard patterns were used to identify retinotopic visual areas of each observer (*SI Text*). Windowed, contrast-reversing (7.5 Hz) sinusoidal luminance gratings at 2 cycles per degree and oriented at 45 ± θ° from the vertical served as stimuli in the experiments. The window was a 5–7° annulus, centered around the fixation point, with 0.2° linear ramps on both the inner and outer edges (Fig. S1*a*). A fixation ''+,'' a square cue, 0.3° × 0.3° in size, and the letters T and L (both 0.29° × 0.48°) also served as display items in the center of the display.

Procedure. In both experiments, each trial started with a 50-ms cue and a 450-ms blank screen (Fig. S1). A small red cue square in the center of a slightly larger dark gray square signaled a central task trial, and a small dark gray cue square on a slightly larger red square signaled a peripheral task trial. In a fixation trial, the fixation display (a ''+'' at the center of a blank screen) was presented throughout the whole trial; no response was made. The task cue was followed by simultaneous presentations (100 ms) of a grating stimulus in the annulus and either a masked T or L at the center of the display and then a 2.4-s fixation screen in Experiment 1 and a 1.4-s fixation screen in Experiment 2. Auditory feedback followed each response. We also monitored eye movements in the scanner using an infrared eye tracker with remote optics (ASL 504 LRO).

Design. We used a block design and an annulus display, identical to that for the main experiments, to localize the ROIs. Each block consisted of 6 s of windowed gratings at 100% contrast followed by 6 s of a blank screen at mean luminance (*SI Text*).

Experiment 1A used a mixed design in which each run consisted of six blocks of alternating central (T or L) and peripheral (±5° from 45°) task conditions, with 26 trials of 3 s each per block (*SI Text*). The task cue was the same in every block. Within each block, 25 trials were evenly divided across four stimulus contrasts (0%, 3%, 30%, and 100%) and one fixation condition; one extra trial in the beginning of each block was included for counterbalancing purposes. There were a total of 156 trials, preceded and followed by a 20-s fixation display. The order of the blocks and all of the contrast conditions within each block were counterbalanced (45). Each scan session consisted of one structural MRI and six functional runs. Each observer participated in one session of data collection. A session lasted ≈1 h.

In Experiment 1A, the desire to have enough blocks in each run and counterbalancing of conditions within each block limited the number of contrast conditions. In Experiment 1B, a rapid event-related design was used to sample CRFs in more contrast conditions. Unlike Experiment 1A, the central and peripheral tasks occurred in separate runs. Six grating contrast conditions, 0%, 1%, 3%, 10%, 30%, and 100%, and one fixation condition were included in each event-related run. Each run consisted of a total of 148 trials. Excluding the first filler trial, there were 21 trials for each condition. Each trial lasted 3 s. These trials were preceded and followed by a 20-s fixation display. The order of the conditions was counterbalanced. Each scan session consisted of one structural MRI and five functional runs of a single (central letter or peripheral grating) task. The order of the two tasks was counterbalanced across observers. Each observer participated in two sessions of data collection. A session lasted ≈1 h.

The event-related design was used in Experiment 2. There were two types of runs with identical stimuli but different task instructions: In the central task runs, observers were asked to identify the letter at the center of the display; in the peripheral task runs, observers were asked to identify whether the orientation of the grating in the periphery was ±θ° from 45°. While the grating contrast was kept constant, four θ conditions, 1°, 2°, 5°, and 10°, and one fixation condition were included in each event-related run. Each run consisted of a total of 127 trials of 2 s each, 25 trials for each condition proceeded by two filler trials. These trials were preceded and followed by an 8-s fixation display. The order of the conditions was counterbalanced. Each session consisted of one structural MRI and eight functional runs. The order of the two tasks (the central letter task and the peripheral orientation task) was counterbalanced within each session. Each observer participated in two sessions of data collection, each with a constant grating contrast (1.9% and 19%). In the 19% condition, no mask was used in the central task. A session lasted ≈1 h.

Data Analyses. All MRI- and fMRI-related data analyses were performed by using a combination of BrainVoyager QX (Brain Innovation) and in-house Matlab programs. All of the fMRI data were first preprocessed to correct for slice timing and head movement, followed by high-pass temporal filtering (cutoff: 3 cycles per run) and removal of linear drift. The 2D functional images were aligned to the 3D structural images in the same session and transformed into the Talairach space. Data from multiple sessions were coregistered through alignment of the structural images from those sessions. Additional curve-fitting and statistical analyses were performed in Matlab.

The BOLD responses to the gratings were obtained in five visual areas, V1, V2, V3, V3A, and V4, in both the central letter (''unattended'') and the peripheral grating (''attended'') conditions. The BOLD signal in each run was normalized by a percent-signal-change transform. The normalized BOLD time series for each subject in each ROI were modeled with a general linear model using the best fitting difference of gamma function as the shape of the HRF with the constraints that $d_1 = a_1 b_1$ and $d_2 = a_2 b_2$ (46):

$$h(t|contrast,attention) = \beta(contrast,attention)h_0(t)$$

$$h_0(t) = \frac{1}{\max(h_0(t))}\left[\left(\frac{t}{d_1}\right)^{a_1}\exp\left(\frac{-(t-d_1)}{b_1}\right) - g\left(\frac{t}{d_2}\right)^{a_2}\exp\left(\frac{-(t-d_2)}{b_2}\right)\right]. \quad [2]$$

The shape of the HRF in an ROI was constrained to be the same in all of the contrast and attention conditions for each subject; the amplitude β(*contrast*,*attention*) was estimated for each contrast and attention condition. To model the mixed design data from Experiment 1A, a block factor was included in the attended block in the general linear model in addition to the trial-by-trial HRF predictors. The procedure combines deconvolution and HRF curve fitting into one single step. Data from Experiment 1A and 1B were first analyzed separately and had virtually identical trial-by-trial CRFs. They were then combined in a joint analysis. The shapes of the HRFs obtained from Experiment 1 were used to estimate the amplitude of the BOLD responses in Experiment 2 with a deconvolution procedure. The aggregate CRFs in each attention condition in each ROI are the average of the amplitudes of the HRFs across subjects.

All the fitting procedures were implemented in Matlab using a nonlinear least-square method. The goodness of fit was evaluated by the r^2 statistic. Different variants of the models were compared by using an *F* test for nested models (*SI Text*).

ACKNOWLEDGMENTS. We thank Dr. Jiancheng Zhuang for his help with data collection. This research was supported by National Science Foundation Grant HD29891 (to Z.-L.L.) and National Institutes of Health Grant EY016391 (to B.S.T.).

1. Shiffrin RM (1988) in *Stevens' Handbook of Experimental Psychology*, eds Atkinson RC, Herrnstein RJ, Lindzey G, Luce R (Wiley, Oxford), 2nd Ed, pp 739–811.
2. Posner MI, Nissen MJ, Ogden WC (1978) in *Modes of Perceiving and Processing Information*, eds Pick NHL, Saltzman IJ (Erlbaum, Hillsdale, NJ), pp 137–157.
3. Brefczynski JA, DeYoe EA (1999) A physiological correlate of the ''spotlight'' of visual attention. *Nat Neurosci* 2:370–374.
4. Gandhi SP, Heeger DJ, Boynton GM (1999) Spatial attention affects brain activity in human primary visual cortex. *Proc Natl Acad Sci USA* 96:3314–3319.
5. Kanwisher N, Wojciulik E (2000) Visual attention: Insights from brain imaging. *Nat Rev Neurosci* 1:91–100.
6. Kastner S, Pinsk MA, De Weerd P, Desimone R, Ungerleider LG (1999) Increased activity in human visual cortex during directed attention in the absence of visual stimulation. *Neuron* 22:751–761.
7. Martinez A, *et al.* (1999) Involvement of striate and extrastriate visual cortical areas in spatial attention. *Nat Neurosci* 2:364–369.
8. Somers DC, Dale AM, Seiffert AE, Tootell RBH (1999) Functional MRI reveals spatially specific attentional modulation in human primary visual cortex. *Proc Natl Acad Sci USA* 96:1663–1668.

9. Watanabe T, *et al.* (1998) Attention-regulated activity in human primary visual cortex. *J Neurophysiol* 79:2218–2221.
10. O'Connor DH, Fukui MM, Pinsk MA, Kastner S (2002) Attention modulates responses in the human lateral geniculate nucleus. *Nat Neurosci* 5:1203–1209.
11. Giesbrecht B, Weissman DH, Woldorff MG, Manqun GR (2006) Pre-target activity in visual cortex predicts behavioral performance on spatial and feature attention tasks. *Brain Res* 1080:63–72.
12. Ress D, Backus BT, Heeger DJ (2000) Activity in primary visual cortex predicts performance in a visual detection task. *Nat Neurosci* 3:940–945.
13. Liu TS, Pestilli F, Carrasco M (2005) Transient attention enhances perceptual performance and fMRI response in human visual cortex. *Neuron* 45:469–477.
14. Serences JT, *et al.* (2005) Coordination of voluntary and stimulus-driven attentional control in human cortex. *Psychol Sci* 16:114–122.
15. Silver MA, Ress D, Heeger DJ (2005) Topographic maps of visual spatial attention in human parietal cortex. *J Neurophysiol* 94:1358–1371.
16. Lu Z-L, Dosher BA (2008) Characterizing observer states using external noise and observer models: Assessing internal representations with external noise. *Psychol Rev* 115:44–82.
17. Lu Z-L, Dosher BA (1998) External noise distinguishes attention mechanisms. *Vision Res* 38:1183–1198.
18. Williford T, Maunsell JH (2006) Effects of spatial attention on contrast response functions in macaque area V4. *J Neurophysiol* 96:40–54.
19. Reynolds JH, Pasternak T, Desimone R (2000) Attention increases sensitivity of V4 neurons. *Neuron* 26:703–714.
20. Lee DK, Itti L, Koch C, Braun J (1999) Attention activates winner-take-all competition among visual filters. *Nat Neurosci* 2:375–381.
21. Tolhurst DJ, Movshon JA, Thompson ID (1981) The dependence of response amplitude and variance of cat visual cortical-neurons on stimulus contrast. *Exp Brain Res* 41:414–419.
22. Engel SA, *et al.* (1994) fMRI of human visual-cortex. *Nature* 369:525–525.
23. Sereno MI, *et al.* (1995) Borders of multiple visual areas in humans revealed by functional magnetic-resonance-imaging. *Science* 268:889–893.
24. Boynton GM, Demb JB, Glover GH, Heeger DJ (1999) Neuronal basis of contrast discrimination. *Vision Res* 39:257–269.
25. Buracas GT, Boynton GM (2007) The effect of spatial attention on contrast response functions in human visual cortex. *J Neurosci* 27:93–97.
26. Gardner JL, *et al.* (2005) Contrast adaptation and representation in human early visual cortex. *Neuron* 47:607–620.
27. Murray SO, He S (2006) Contrast invariance in the human lateral occipital complex depends on attention. *Curr Biol* 16:606–611.
28. Olman CA, Ugurbil K, Schrater P, Kersten D (2004) BOLD fMRI and psychophysical measurements of contrast response to broadband images. *Vision Res* 44:669–683.
29. Martinez-Trujillo JC, Treue S (2002) Attentional modulation strength in cortical area MT depends on stimulus contrast. *Neuron* 35:365–370.
30. Morrone MC, Denti V, Spinelli D (2004) Different attentional resources modulate the gain mechanisms for color and luminance contrast. *Vision Res* 44:1389–1401.
31. Huang LQ, Dobkins KR (2005) Attentional effects on contrast discrimination in humans: Evidence for both contrast gain and response gain. *Vision Res* 45:1201–1212.
32. Ling S, Carrasco M (2006) Sustained and transient covert attention enhance the signal via different contrast response functions. *Vision Res* 46:1210–1220.
33. Naka KI, Rushton WA (1966) S-potentials from colour units in the retina of fish (Cyprinidae). *J Physiol (London)* 185:536–555.
34. Boynton GM, Demb JB, Heeger DJ (1996) Neural basis of contrast appearance measured with fMRI. *Invest Ophthalmol Visual Sci* 37:4210–4210.
35. Backus BT, Fleet DJ, Parker AJ, Heeger DJ (2001) Human cortical activity correlates with stereoscopic depth perception. *J Neurophysiol* 86:2054–2068.
36. Huk AC, Heeger DJ (2000) Task-related modulation of visual cortex. *J Neurophysiol* 83:3525–3536.
37. Ress D, Heeger DJ (2003) Neuronal correlates of perception in early visual cortex. *Nat Neurosci* 6:414–420.
38. Blaser E, Sperling G, Lu ZL (1999) Measuring the amplification of attention. *Proc Natl Acad Sci USA* 96:11681–11686.
39. Carrasco M, Penpeci-Talgar C, Eckstein M (2000) Spatial covert attention increases contrast sensitivity across the CSF: Support for signal enhancement. *Vision Res* 40:1203–1215.
40. Heeger DJ, Ress D (2002) What does fMRI tell us about neuronal activity? *Nat Rev Neurosci* 3:142–151.
41. Logothetis NK, Pauls J, Augath M, Trinath T, Oeltermann A (2001) Neurophysiological investigation of the basis of the fMRI signal. *Nature* 412:150–157.
42. Buracas GT, Fine I, Boynton GM (2005) The relationship between task performance and functional magnetic resonance imaging response. *J Neurosci* 25:3023–3031.
43. Maunsell JHR, Cook EP (2002) The role of attention in visual processing. *Philos Trans R Soc London Ser B* 357:1063–1072.
44. Felleman DJ, Van Essen DC (1991) Distributed hierarchical processing in the primate cerebral cortex. *Cereb Cortex* 1:1–47.
45. Kourtzi Z, Kanwisher N (2001) Representation of perceived object shape by the human lateral occipital complex. *Science* 293:1506–1509.
46. Friston KJ, *et al.* (1998) Event-related fMRI: Characterizing differential responses. *NeuroImage* 7:30–40.

Supporting Information

Li *et al.* 10.1073/pnas.0801390105

SI Text

Retinotopy and ROI. ***Stimuli.*** Wedges and rings made of flickering radial color checker-board patterns were used to identify retinotopic visual areas of each observer. The aspect ratio of the checkers was kept constant by setting their (radial) height equal to their (tangential) mid-width. Four color combinations were used to create the checker-board patterns: black and white, red and cyan, green and purple, and blue and yellow. The display cycled through eight different images per second, consisting of a reversal of each of the four color combinations. The wedge, with an 8.5° radius and a width of one-eighth of a disk, rotated counterclockwise one-fourth of its width per second, so it swept the whole visual field in 32 s. Each ring was made of two checkers in the radial direction. The rings expanded from the center of the display at the speed of one checker per second. The entire cycle took 20 s. The fixation of the display changed from "+" to "×" or vice versa in randomly chosen intervals between 5 and 15 s. ***Procedure.*** In the retinotopy session, observers maintained fixation while viewing rotating wedges, expanding rings, or a flickering annulus. To help them maintain fixation, observers were required to press a key on the MRI-compatible response button box as soon as a change of the fixation mark was detected. A block design was used to measure the retinotopy and the visual cortical regions associated with the stimuli used in the main experiment (regions of interest, ROIs) for each observer before the main experiments. The retinotopy session consisted of one structural MRI run, and two runs of each of the three stimuli: the wedges, the rings, and the annulus used in the main experiment. The wedges and rings allowed us to separate different visual areas.

Data analysis. Gray-white matter segmentation was performed on the 3D structural images for each observer after image intensity inhomogeneity correction and Talairach spatial normalization. The resulting gray-white matter boundaries were used to create a 3D surface model of the brain, which was then inflated to display both sulci and gyri on smooth surfaces. For each hemisphere, a 2D flat cortical map was then created by unfolding the inflated 3D surface around the mid-brain after cutting it in several places, including one along the calcarine sulcus (left edge of cortical sheet in Fig. S1 *b* and *c*). The flat maps involved minimal areal distortions of the 3D data (≈13%).

Polar angle and eccentricity maps were created by (*i*) computing the average fMRI time series of each voxel across multiple wedge and ring runs, (*ii*) calculating the correlation between the measured BOLD time series and the predicted hemodynamic functions (1), and (*iii*) plotting the correlation map ($r > 0.25$) on a flattened representation of visual cortex (Fig. S1*b*). Boundaries between visual areas were delineated using field-sign mapping, which identifies direction reversals of the polar-angle trajectories and is roughly perpendicular to the eccentricity trajectories on the flat visual area maps (2, 3). Manual adjustment was performed when necessary. The retinotopic regions (V1, V2, V3, V3A, and V4) were defined according to the standard convention. For V4, we included the full hemifield (4). Voxels on the retinotopic map that were also activated by the annulus defined the ROI: Subsections of V1, V2, V3, V3A, and V4 (Fig. S1*c*). The corresponding voxels in the fMRI data were used for all of the subsequent ROI analysis.

Comments on the Attention Manipulation and the Mixed Design. To maximize the observed effects of attention on the BOLD response, we have chosen a "categorical" manipulation of covert attention. The observed effects of attention may reflect the impact of a mixture of spatial and feature attention. The duration of each block in this mixed-design is 78 s, significantly longer than the typical block duration used in most fMRI experiments. Drift for EPI scans on our scanner is minimal and linear in time and removed in preprocessing steps. We were bounded by the constraints imposed by the demands of counterbalancing (a minimum of 26 trials per block) and BOLD linearity assumption (3 s per trial). The resulting design was a reasonable compromise. The relatively long block duration did not cause any major issues because the trial-by-trial results from the mixed design and the event-related design are virtually the same.

Model Selection via Nested Model Tests. Different variants of the Naka-Rushton models were compared using an F-test for nested models. A nested model is one that is a special case of another model in which one of more parameters are equated or fixed. As indicated in the article, the Naka-Rushton equation was fit to the BOLD contrast response functions (CRFs) in each cortical region:

$$R(c) = b + \frac{R_{\max} c^2}{c_{50}^2 + c^2}, \qquad [1]$$

where c is the contrast of the grating, b is the baseline activity, c_{50} denotes the contrast at which the response reaches half of its maximum dynamic range, and $R_{\max}$ is the maximum response above the baseline. For each cortical region, a model is fit simultaneously to the data for the attended and the unattended conditions. In the most saturated model, the attended and unattended condition may differ in all three aspects (b, c_{50}, and $R_{\max}$) (i.e., two N-R equations with independent estimates of all three parameters). Nested special cases are those in which, for example, the baseline b is assumed to be identical for the attended and unattended condition, and so on. A (nested) reduced model, which is a special case of a fuller model, is tested for significance using the nested F test:

$$F = \frac{(RSS_{\text{reduced}} - RSS_{\text{full}})}{(k_{\text{full}} - k_{\text{reduced}})} \Big/ \frac{(RSS_{\text{full}})}{(k_{\text{full}})},$$

with degrees of freedom $k_{\text{full}} - k_{\text{reduced}}$ and $n - k_{\text{full}}$. The RSS is the residual sum of squared errors for the model (5). The F-statistic compares the mean squared errors per each added parameter in the fuller model to the mean squared errors for each remaining degree of freedom after prediction by the fuller model. In other words, the test evaluates whether the variance accounted for by the added parameters in the fuller model is significantly larger than expected by chance. If so, then the added parameter in the fuller model expresses a significant difference between conditions. A lattice of such nested models may be used to identify the model that best accounts for the data with the fewest (significantly different) parameters.

The Bootstrap Procedure. To evaluate the effect of individual differences on the model selection results, we conducted a statistical study with the following bootstrap procedure: (*i*) Sampling with replacement the estimated CRFs from six observers. The entire set of CRFs from the five ROIs and attention conditions of each subject was treated as a single unit in the sampling procedure. (*ii*) As with the original data set, the six sets of re-sampled CRFs were averaged, separately for each ROI and

attention conditions and weighted by the standard errors of each BOLD response. (*iii*) The full model lattice based on the modified Naka-Rushton equation was fitted to the average CSFs. (*iv*) The best fitting model, the one that is not significantly different from the most saturated but superior to all its reduced models, was selected. (*v*) Steps *i–iv* were repeated one million times. (*vi*) The frequency of each candidate model as the best fitting model was computed. The standard deviations of the parameters of the baseline plus contrast-gain model were also computed using the bootstrapped samples.

Eye Movement Results. The eye-tracking data from two observers were analyzed. Fixation state was quantified along several dimensions: horizontal and vertical eye position during fixation, fixation duration, number of blinks per trial, number of saccades per trial, and saccade amplitude. Only horizontal eye position showed any significant difference between the two attention conditions [$F(1,1) = 422$, $P < 0.05$). The eyes were shifted horizontally away from fixation by an average of 0.13° in the attended (periphery) condition, which was less than 3% of the distance to the inner edge of the grating annulus—too small to be responsible for the observed behavioral or physiological differences between the attended and unattended conditions.

Effects of Attention at Other Eccentricities. The aggregated CRFs of the five cortical regions in the attended and unattended were measured at four additional eccentricities: fovea (0–2°), inner annulus 1 (3.6–4.2°), inner annulus 2 (4.2–5°), and an outer annulus (7–7.8°). In fovea, attending to the grating stimulus reduced the BOLD responses from 11.8% to 7.1%, independent of the grating contrast. In inner annuli 1 and 2, the BOLD response didn't depend on grating contrast but was increased by attention. In the outer annulus, the shapes of the BOLD CRFs and the effect of attention are very similar to those in the stimulus annulus.

The Shape of the BOLD CRFs. The BOLD CRFs in the early visual areas in the current study exhibited saturation at relatively low signal contrast, particularly in the attended condition. This is consistent with several other event-related BOLD CRF studies using brief stimuli (6, 7). In contrast, BOLD CRFs in several block-design studies showed either little saturation or saturation in much higher signal contrasts (8–10). The saturation points in the event-related and block designs may differ due to the different stimulus durations, contrast adaptation levels, and perhaps attentional states.

1. Boynton GM, Demb JB, Heeger DJ (1996) Neural basis of contrast appearance measured with fMRI. *Invest Ophthalmol Visual Sci* 37:4210–4210.
2. Engel SA, Glover GH, Wandell BA (1997) Retinotopic organization in human visual cortex and the spatial precision of functional MRI. *Cereb Cortex* 7:181–192.
3. Sereno MI, *et al.* (1995) Borders of multiple visual areas in humans revealed by functional magnetic-resonance-imaging. *Science* 268:889–893.
4. Wandell BA, Brewer AA, Dougherty RF (2005) Visual field map clusters in human cortex. *Philos Trans R Soc London Ser B* 360:693–707.
5. Wonnacott TH, Wonnacott RJ (1981) *Regression: A Second Course in Statistics* (Wiley, New York).
6. Gardner JL, *et al.* (2005) Contrast adaptation and representation in human early visual cortex. *Neuron* 47:607–620.
7. Murray SO, He S (2006) Contrast invariance in the human lateral occipital complex depends on attention. *Curr Biol* 16:606–611.
8. Avidan G, *et al.* (2002) Contrast sensitivity in human visual areas and its relationship to object recognition. *J Neurophysiol* 87:3102.
9. Boynton GM, Demb JB, Glover GH, Heeger DJ (1999) Neuronal basis of contrast discrimination. *Vision Res* 39:257–269.
10. Olman CA, Ugurbil K, Schrater P, Kersten D (2004) BOLD fMRI and psychophysical measurements of contrast response to broadband images. *Vision Res* 44:669–683.

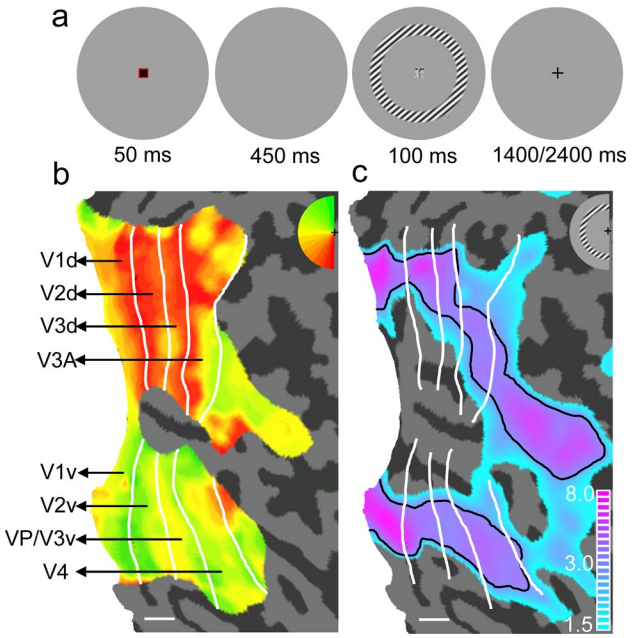

Fig. S1. Stimulus and regions of interest. (*a*) Display sequence of a typical trial. (*b*) The retinotopy of a typical subject. The colors denote significant activations by the wedge stimulus in the different sectors of the visual field, as illustrated by the half-disk at the upper right corner. (*c*) Regions of interest, demarcated by the black lines ($t \geq 3$, $P < 0.003$) and boundaries of visual areas (the white lines). Different t values are illustrated using different colors. (Scale bars: 1 cm on the flattened cortical surface.)